Tests of GR from LIGO-Virgo detections

Archisman Ghosh
Nikhef, Amsterdam

COST Action Gravity Data Group Meeting
Athens, 2019 January 16

Nikhef

International Centre for Theoretical Sciences
Tata Institute of Fundamental Research

LSC VIRGO

Plan of talk

Orientation and basics of LIGO-Virgo data analysis

Searches $\longrightarrow$ parameter estimation $\longrightarrow$ science implications

Testing general relativity

Results with O1 and O2 detections

Future prospects and plans

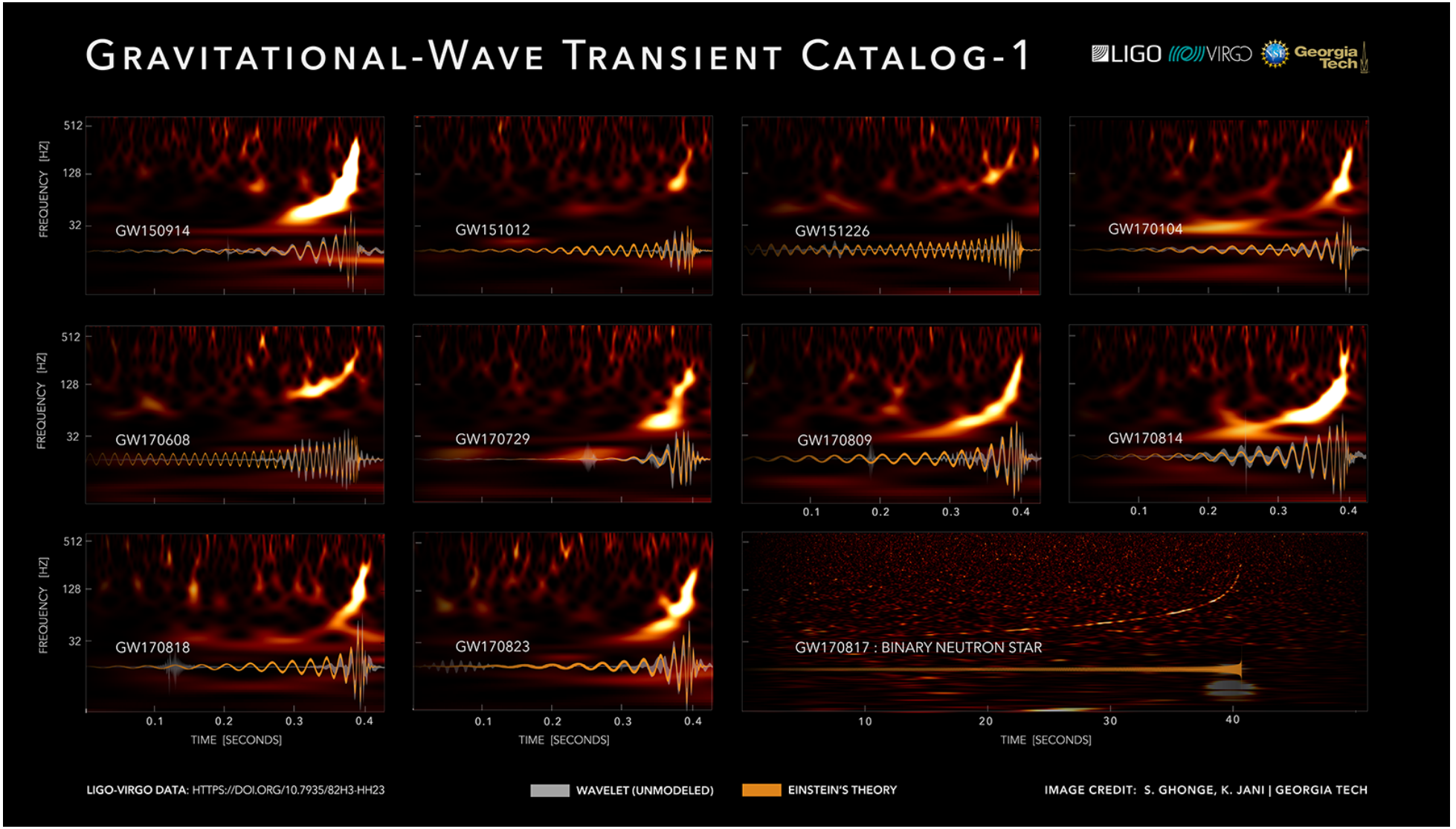
GRAVITATIONAL-WAVE TRANSIENT CATALOG-1
LIGO VIRGO Georgia Tech
FREQUENCY [HZ]
512
128
32
GW150914
GW151012
GW151226
GW170104
GW170608
GW170729
GW170809
GW170814
GW170818
GW170823
GW170817 : BINARY NEUTRON STAR
0.1
0.2
0.3
0.4
10
20
30
40
TIME [SECONDS]
LIGO-VIRGO DATA: HTTPS://DOI.ORG/10.7935/82H3-HH23
WAVELET (UNMODELED)
EINSTEIN'S THEORY
IMAGE CREDIT: S. GHONGE, K. JANI | GEORGIA TECH

LIGO-Virgo data analysis

	Long-duration	Transient
Unmodelled	Stochastic background Cosmological + BBH	Bursts Supernova explosions
Modelled	Continuous waves Spinning deformed NS	Compact binary coalescences NS-NS, NS-BH, BBH

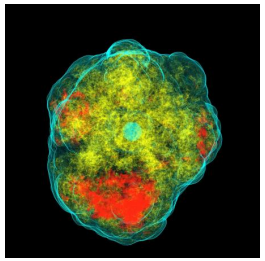

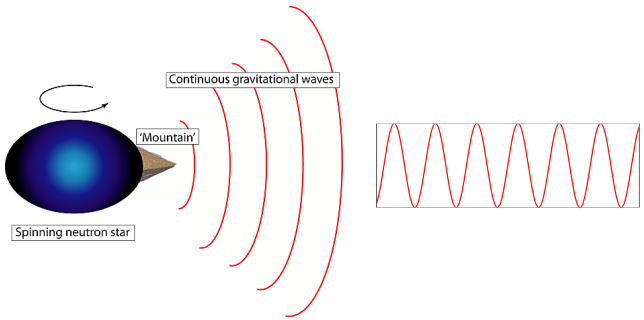

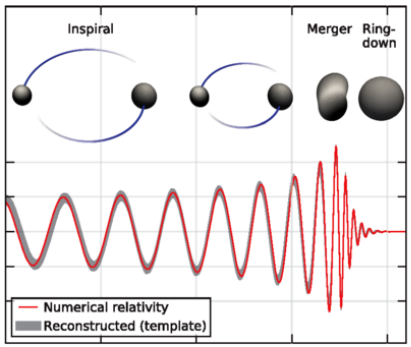

Data analysis of CBCs

Searches

Generate (real-time) triggers

Abbott *et al.*, PRX **6**, 041015 (2016)

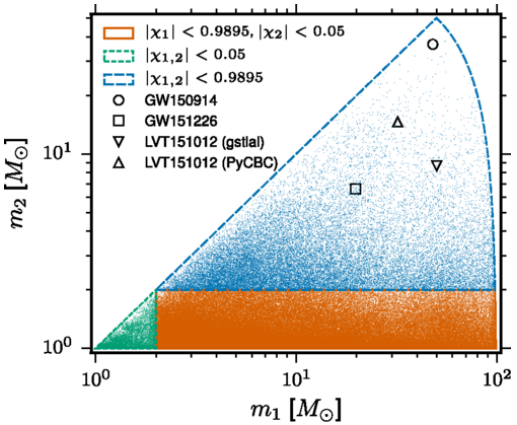

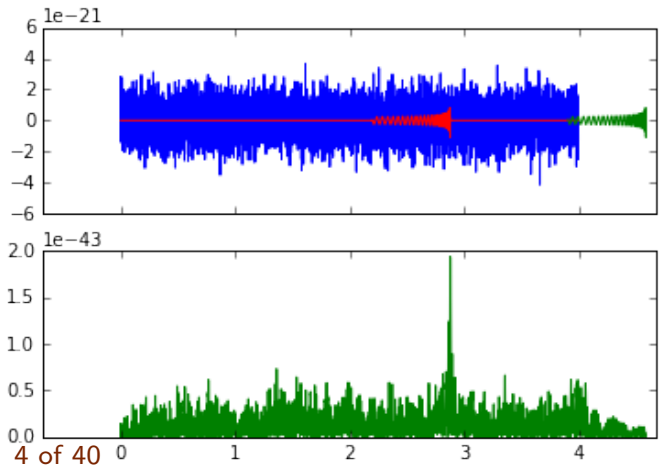

Parameter estimation

Rigorous analysis of data around trigger

Low latency

quick

BayesSTAR

RapidPE

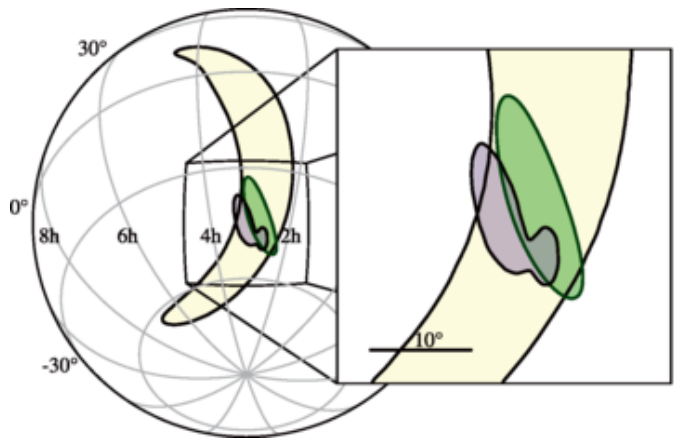

Implications

Fundamental physics, astrophysics, cosmology

High latency

accurate

LALInference

Searches

MATCHED FILTERING

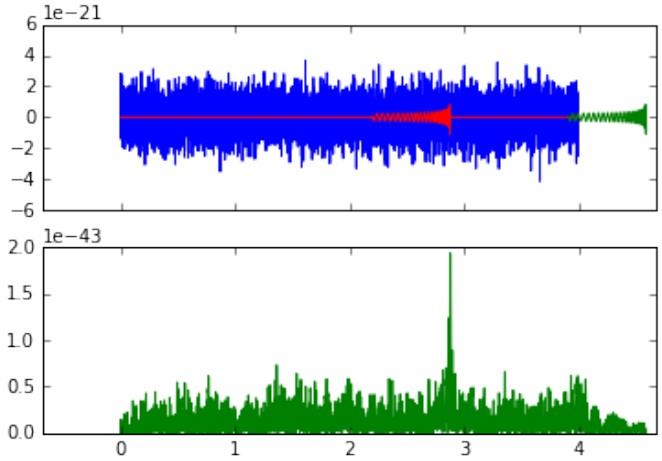

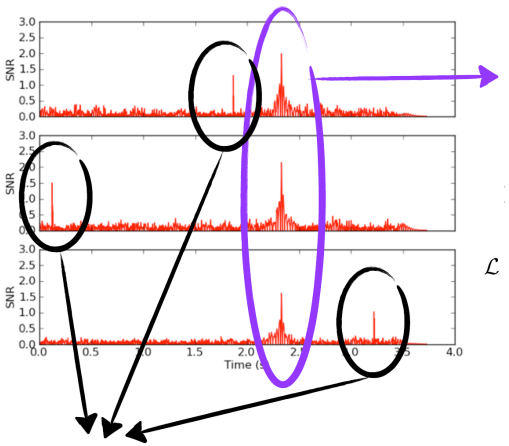

BACKGROUND

COINCIDENT TRIGGERS

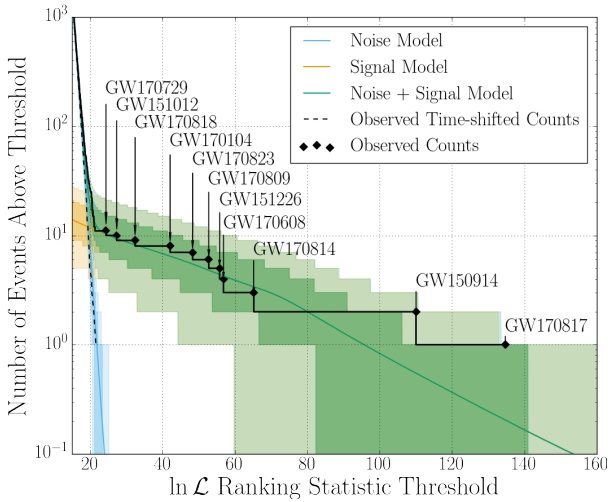

Abbott *et al.* arXiv:1811.12907 [astro-ph.HE]

RANKING & SIGNIFICANCE

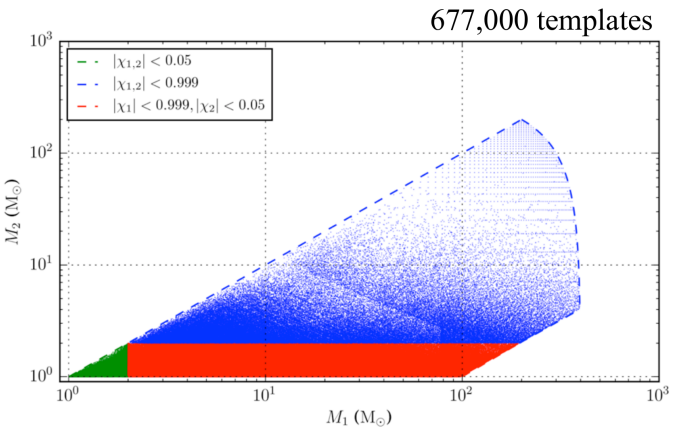

O2 TEMPLATE BANK

Event	Network SNR GstLAL
GW150914	24.4
GW151012	10.0
GW151226	13.1
GW170104	13.0
GW170608	14.9
GW170729	10.8
GW170809	12.4
GW170814	15.9
GW170817	33.0
GW170818	11.3
GW170823	11.5

The waveform template

Analytical parametric description of GW solutions in GR:

$$h(f;\mathbf{\Omega}) = A(f;\mathbf{\Omega})e^{i\Phi(f;\mathbf{\Omega})}$$
$$\Phi(f;\mathbf{\Omega}) = \Phi(f; m_1, m_2, \vec{s_1}, \vec{s_2})$$

Modelled by a combination of:

- Post-Newtonian theory (early inspiral)
- Numerical relativity (merger)
- Black hole perturbation theory (ringdown)

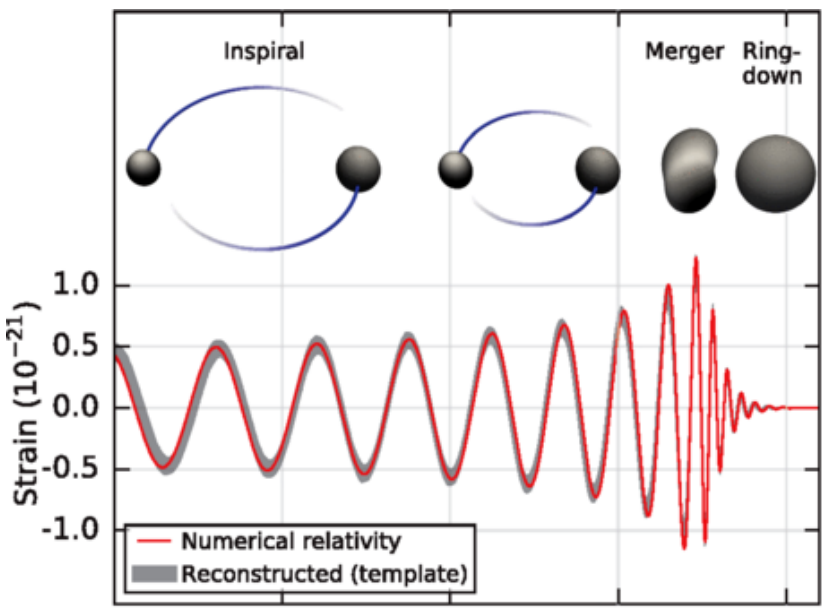

Phenom (hybrid) **EOB**

Intrinsic parameters

- Component masses, $m_{1,2}$
- Component dimensionless spin angular momenta, $\vec{s}_{1,2}$
- Tidal parameters for neutron stars, $\lambda_{1,2}$
- Any residual eccentricity?

$$\vec{s} \equiv \frac{\vec{J}}{m^2}$$

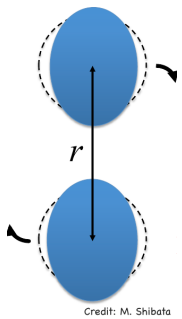

Neutron stars in binaries are tidally deformed.

Have a measurable effect on the orbital motion.

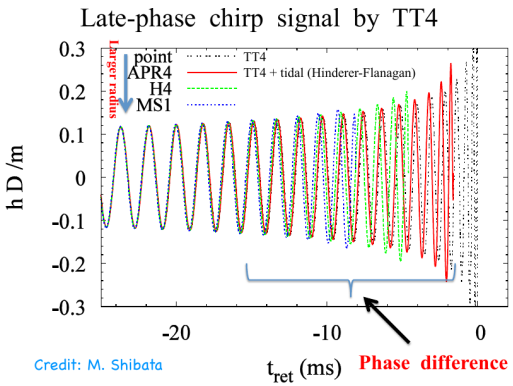

Two polarizations

Dominant $(2,2)$-mode to leading order:

$$h_+(t) = \frac{2M\eta}{D}(\pi M f_{\rm GW})^2(1+\cos^2\iota)\cos 2\phi(t)$$

$$h_\times(t) = \frac{4M\eta}{D}(\pi M f_{\rm GW})^2\cos\iota\sin 2\phi(t)$$

$$M \equiv m_1 + m_2 \qquad \eta \equiv \frac{m_1 m_2}{M^2}$$

- Distance, D
- Inclination angle, ι
- Phase at coalescence, ϕ_c
- Time of coalescence, t_c

Antenna beam pattern functions

- Polarization angle, ψ: $h = F_+ h_+ + f_\times h_\times$
- Two angles in the sky $(\theta, \phi) \longrightarrow (\alpha, \delta)$, right ascension and declination

$$F_+(\theta, \phi, \psi) = -\frac{1}{2}(1 + \cos^2\theta)\cos 2\phi \cos 2\psi - \cos\theta \sin 2\phi \sin 2\psi \quad \text{(A.10)}$$

$$F_\times(\theta, \phi, \psi) = +\frac{1}{2}(1 + \cos^2\theta)\cos 2\phi \sin 2\psi - \cos\theta \sin 2\phi \cos 2\psi \ . \quad \text{(A.11)}$$

These beam pattern functions are shown in Figure A.1.

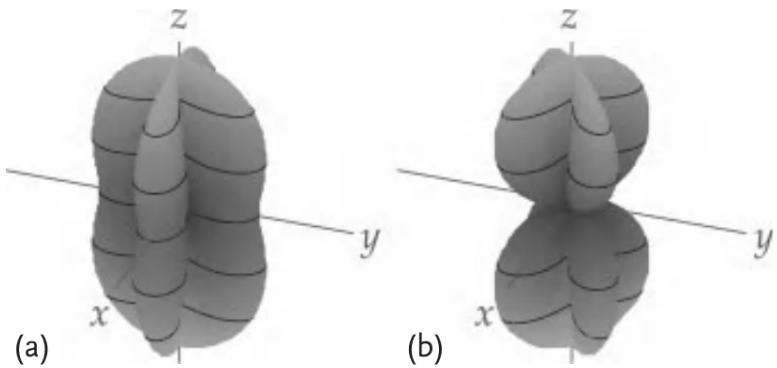

Figure A.1 The beam pattern functions $F_+^2(\theta, \phi, \psi = 0)$ (a) and $F_\times^2(\theta, \phi, \psi = 0)$ (b) for an interferometric gravitational-wave detector with orthogonal arms along the *x*- and *y*-axes.

Parameter estimation: what parameters?

Intrinsic parameters: $\{m_1, m_2, \vec{s}_1, \vec{s}_2, \lambda_1, \lambda_2, \ldots\}$

Extrinsic parameters: $\{\alpha, \delta, d_L, \iota, \psi, \phi_c, t_c\}$

15 parameters for BBHs

At least 17 parameters for BNS

phase	$\Rightarrow$	redshifted chirp mass, $\mathcal{M}^z \equiv \frac{(m_1^z m_2^z)^{3/5}}{(m_1^z+m_2^z)^{1/5}}$, very accurately
	$\Rightarrow$	mass ratio, $q \equiv \frac{m_2}{m_1}$, to a reasonable degree; **strongly correlated with spin & tidal**
amplitude	$\Rightarrow$	combination of $\frac{\mathcal{M}^z(1+\cos^2\iota)}{d_L}$, $\frac{\mathcal{M}^z \cos\iota}{d_L}$ **(dominant 22-mode dependence)**
polarisation	$\Rightarrow$	$\cos^2\iota$ poorly
	$\Rightarrow$	d_L to a reasonable degree

Bayesian parameter estimation

Bayesian parameter estimation: obtain the posterior probability distribution on the parameter space given the data and a prior probability distribution.

$$Posterior(\vec{\Omega}|\text{data}, I) = \frac{Prior(\vec{\Omega}|I)\,\mathcal{L}(\text{data}|\vec{\Omega}, I)}{Evidence(\text{data}, I)}$$

$$\vec{\Omega} = \{\mathcal{M}, q, \vec{s_1}, \vec{s_2}, \lambda_1, \lambda_2, \alpha, \sin\delta, d_L, \cos\iota, \psi, \phi_c, t_c\}$$

$$\begin{aligned}\mathcal{L}(\text{data}|\vec{\Omega}, I) &= P(\text{data}|\text{signal}(\vec{\Omega}), I) \\ &= \exp\left(-\frac{1}{2}\left\langle \text{data} - \text{signal}(\vec{\Omega})|\text{data} - \text{signal}(\vec{\Omega})\right\rangle\right)\end{aligned}$$

$\text{data} = \text{signal}(\vec{\Omega}) + \text{noise}, n$

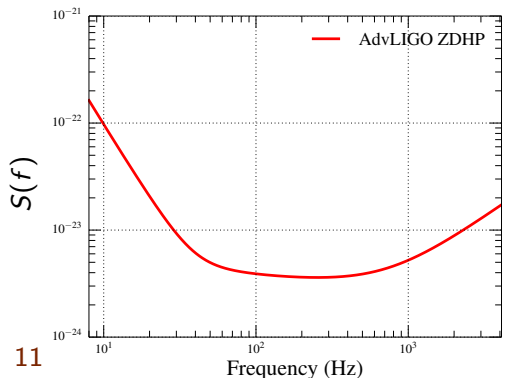

$$\langle n|n\rangle \equiv \int df \frac{||n(f)||^2}{S^2(f)}$$

Gaussian noise

Bayesian model selection

- Compute the odds ratio between various models

$$\mathcal{O}_{12} = \frac{P(\mathcal{H}_1|\mathcal{I})}{P(\mathcal{H}_2|\mathcal{I})} \frac{P(\text{data}|\mathcal{H}_1, \mathcal{I})}{P(\text{data}|\mathcal{H}_2, \mathcal{I})}$$

- Evidence accumulates over multiple detections

GWTC-1: A Gravitational-Wave Transient Catalog of Compact Binary Mergers Observed by LIGO and Virgo during the First and Second Observing Runs

The LIGO Scientific Collaboration and The Virgo Collaboration

(Compiled: 3 December 2018)

Abbott *et al.* arXiv:1811.12907 [astro-ph.HE]

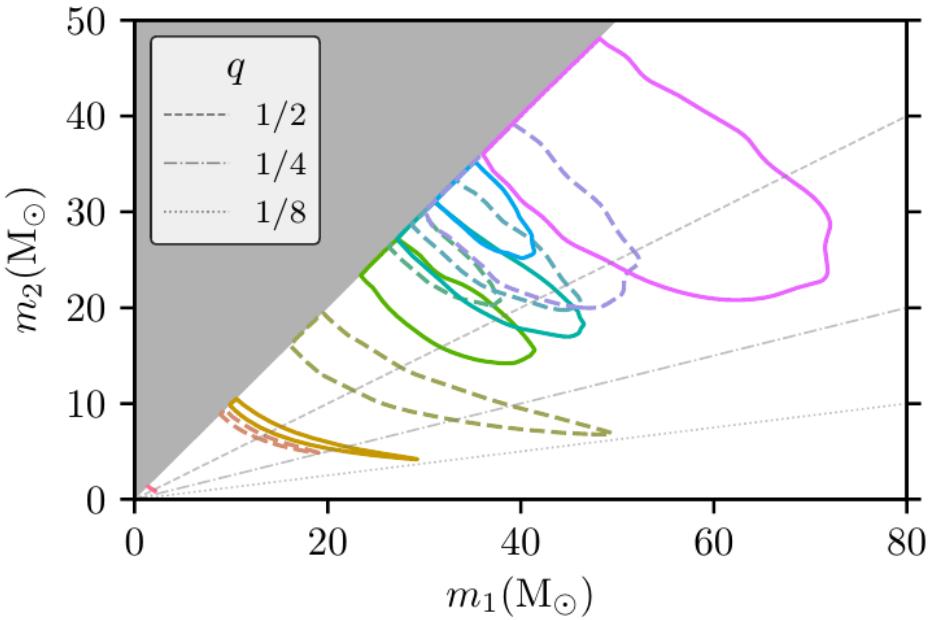

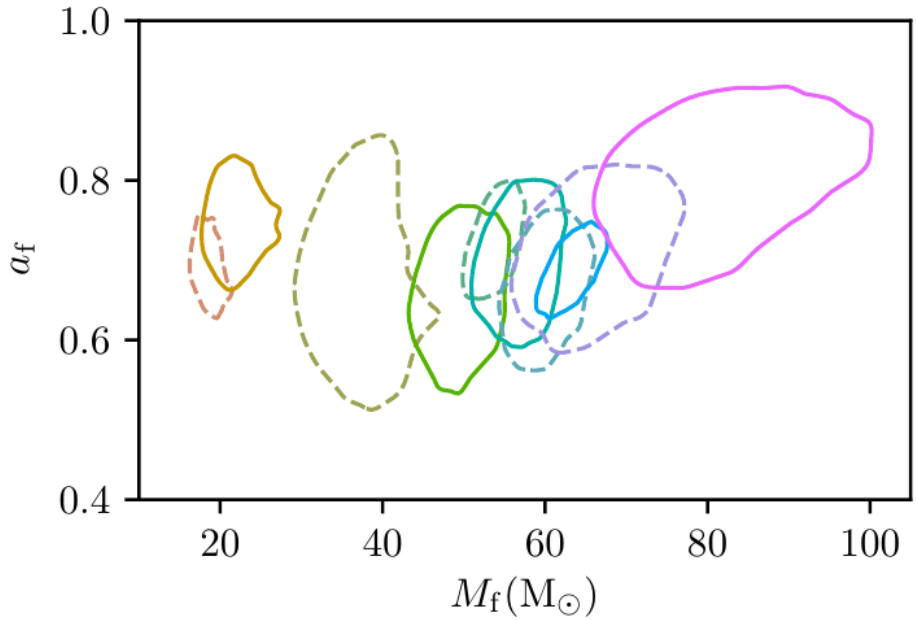

GW170817 GW151226 GW170104 GW170809 GW150914 GW170729
GW170608 GW151012 GW170814 GW170818 GW170823

GWTC-1: A Gravitational-Wave Transient Catalog of Compact Binary Mergers Observed by LIGO and Virgo during the First and Second Observing Runs

The LIGO Scientific Collaboration and The Virgo Collaboration

(Compiled: 3 December 2018)

Abbott *et al.* arXiv:1811.12907 [astro-ph.HE]

Event	$m_1/\mathrm{M}_\odot$	$m_2/\mathrm{M}_\odot$	$\mathcal{M}/\mathrm{M}_\odot$	χ_{eff}	$M_\mathrm{f}/\mathrm{M}_\odot$	a_f	$E_\mathrm{rad}/(\mathrm{M}_\odot c^2)$	$\ell_\mathrm{peak}/(\mathrm{erg\,s}^{-1})$	d_L/Mpc	z	$\Delta\Omega/\mathrm{deg}^2$
GW150914	$35.6^{+4.8}_{-3.0}$	$30.6^{+3.0}_{-4.4}$	$28.6^{+1.6}_{-1.5}$	$-0.01^{+0.12}_{-0.13}$	$63.1^{+3.3}_{-3.0}$	$0.69^{+0.05}_{-0.04}$	$3.1^{+0.4}_{-0.4}$	$3.6^{+0.4}_{-0.4}\times10^{56}$	430^{+150}_{-170}	$0.09^{+0.03}_{-0.03}$	179
GW151012	$23.3^{+14.0}_{-5.5}$	$13.6^{+4.1}_{-4.8}$	$15.2^{+2.0}_{-1.1}$	$0.04^{+0.28}_{-0.19}$	$35.7^{+9.9}_{-3.8}$	$0.67^{+0.13}_{-0.11}$	$1.5^{+0.5}_{-0.5}$	$3.2^{+0.8}_{-1.7}\times10^{56}$	1060^{+540}_{-480}	$0.21^{+0.09}_{-0.09}$	1555
GW151226	$13.7^{+8.8}_{-3.2}$	$7.7^{+2.2}_{-2.6}$	$8.9^{+0.3}_{-0.3}$	$0.18^{+0.20}_{-0.12}$	$20.5^{+6.4}_{-1.5}$	$0.74^{+0.07}_{-0.05}$	$1.0^{+0.1}_{-0.2}$	$3.4^{+0.7}_{-1.7}\times10^{56}$	440^{+180}_{-190}	$0.09^{+0.04}_{-0.04}$	1033
GW170104	$31.0^{+7.2}_{-5.6}$	$20.1^{+4.9}_{-4.5}$	$21.5^{+2.1}_{-1.7}$	$-0.04^{+0.17}_{-0.20}$	$49.1^{+5.2}_{-3.9}$	$0.66^{+0.08}_{-0.10}$	$2.2^{+0.5}_{-0.5}$	$3.3^{+0.6}_{-0.9}\times10^{56}$	960^{+430}_{-410}	$0.19^{+0.07}_{-0.08}$	924
GW170608	$10.9^{+5.3}_{-1.7}$	$7.6^{+1.3}_{-2.1}$	$7.9^{+0.2}_{-0.2}$	$0.03^{+0.19}_{-0.07}$	$17.8^{+3.2}_{-0.7}$	$0.69^{+0.04}_{-0.04}$	$0.9^{+0.0}_{-0.1}$	$3.5^{+0.4}_{-1.3}\times10^{56}$	320^{+120}_{-110}	$0.07^{+0.02}_{-0.02}$	396
GW170729	$50.6^{+16.6}_{-10.2}$	$34.3^{+9.1}_{-10.1}$	$35.7^{+6.5}_{-4.7}$	$0.36^{+0.21}_{-0.25}$	$80.3^{+14.6}_{-10.2}$	$0.81^{+0.07}_{-0.13}$	$4.8^{+1.7}_{-1.7}$	$4.2^{+0.9}_{-1.5}\times10^{56}$	2750^{+1350}_{-1320}	$0.48^{+0.19}_{-0.20}$	1033
GW170809	$35.2^{+8.3}_{-6.0}$	$23.8^{+5.2}_{-5.1}$	$25.0^{+2.1}_{-1.6}$	$0.07^{+0.16}_{-0.16}$	$56.4^{+5.2}_{-3.7}$	$0.70^{+0.08}_{-0.09}$	$2.7^{+0.6}_{-0.6}$	$3.5^{+0.6}_{-0.9}\times10^{56}$	990^{+320}_{-380}	$0.20^{+0.05}_{-0.07}$	340
GW170814	$30.7^{+5.7}_{-3.0}$	$25.3^{+2.9}_{-4.1}$	$24.2^{+1.4}_{-1.1}$	$0.07^{+0.12}_{-0.11}$	$53.4^{+3.2}_{-2.4}$	$0.72^{+0.07}_{-0.05}$	$2.7^{+0.4}_{-0.3}$	$3.7^{+0.4}_{-0.5}\times10^{56}$	580^{+160}_{-210}	$0.12^{+0.03}_{-0.04}$	87
GW170817	$1.46^{+0.12}_{-0.10}$	$1.27^{+0.09}_{-0.09}$	$1.186^{+0.001}_{-0.001}$	$0.00^{+0.02}_{-0.01}$	≤ 2.8	≤ 0.89	≥ 0.04	$\geq 0.1\times10^{56}$	40^{+10}_{-10}	$0.01^{+0.00}_{-0.00}$	16
GW170818	$35.5^{+7.5}_{-4.7}$	$26.8^{+4.3}_{-5.2}$	$26.7^{+2.1}_{-1.7}$	$-0.09^{+0.18}_{-0.21}$	$59.8^{+4.8}_{-3.8}$	$0.67^{+0.07}_{-0.08}$	$2.7^{+0.5}_{-0.5}$	$3.4^{+0.5}_{-0.7}\times10^{56}$	1020^{+430}_{-360}	$0.20^{+0.07}_{-0.07}$	39
GW170823	$39.6^{+10.0}_{-6.6}$	$29.4^{+6.3}_{-7.1}$	$29.3^{+4.2}_{-3.2}$	$0.08^{+0.20}_{-0.22}$	$65.6^{+9.4}_{-6.6}$	$0.71^{+0.08}_{-0.10}$	$3.3^{+0.9}_{-0.8}$	$3.6^{+0.6}_{-0.9}\times10^{56}$	1850^{+840}_{-840}	$0.34^{+0.13}_{-0.14}$	1651

Testing general relativity

Probing strong-field gravity

Abbott *et al.*, PRL **116**, 061102 (2016)

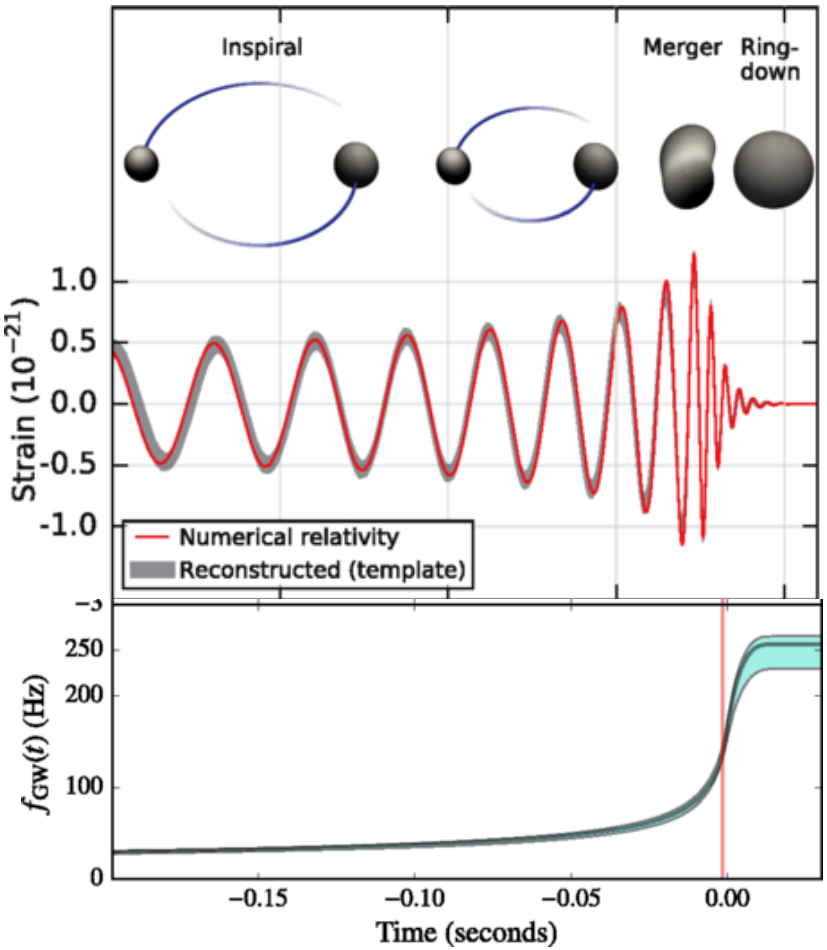

Abbott *et al.*, PRL **116**, 221101 (2016)

PRL **116,** 221101 (2016) | Selected for a Viewpoint in *Physics* PHYSICAL REVIEW LETTERS | week ending 3 JUNE 2016

Tests of General Relativity with GW150914

B. P. Abbott *et al.*[*]

(LIGO Scientific and Virgo Collaborations)

(Received 26 March 2016; revised manuscript received 9 May 2016; published 31 May 2016)

First probes into the dynamical regime of strong field general relativity (GR).

Yunes *et al.* (2016)

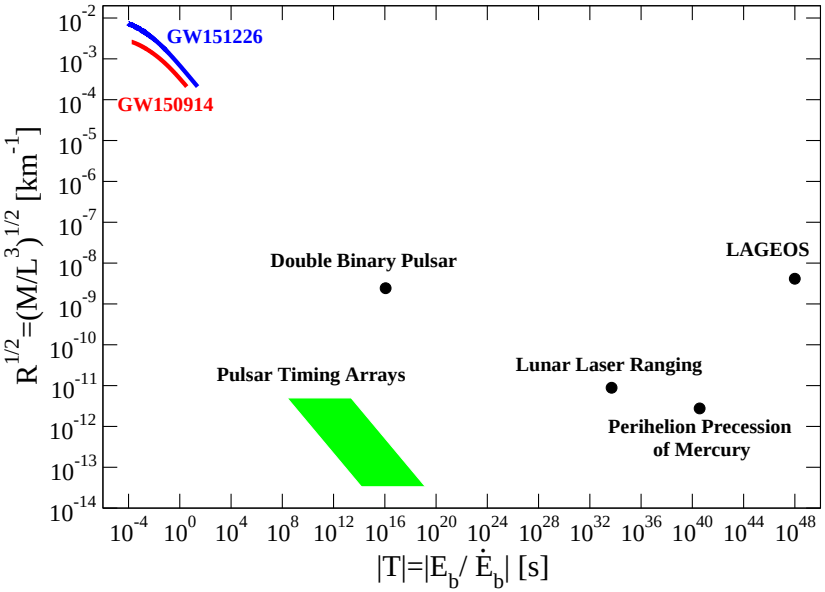

Testing GR: the waveform model

The gravitational waveform carries information about:

- The nature of and properties of the binary
- The non-linear dynamics of spacetime
- The final object

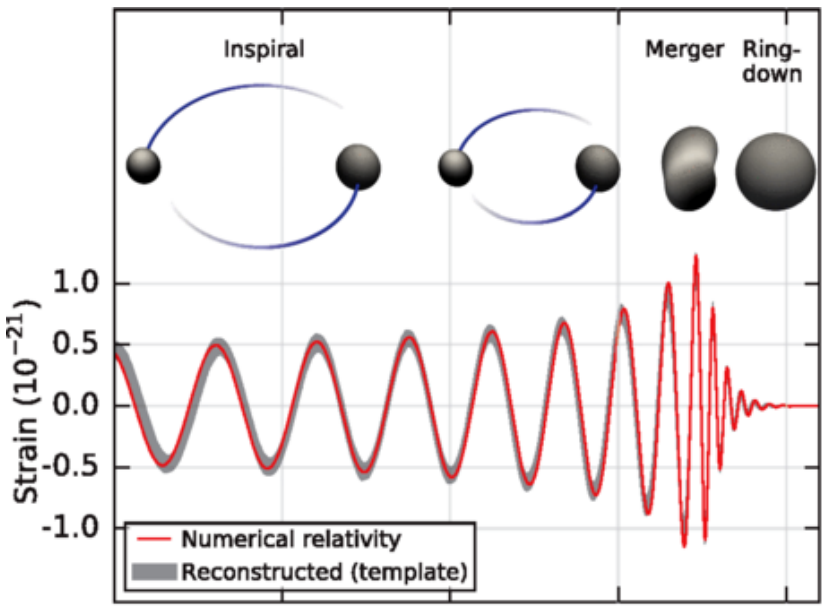

Three roads to testing GR

"Look under the lamppost"

- Consistency: data is described by the waveform (and the noise) model
- Search for generic deformations to the waveform model
- Look for signatures of specific theories

Perform model selection: GR / non-GR?

Residuals

- Residual of the data after subtracting the best-fit waveform is statistically consistent with detector noise at other times when no signal is present.

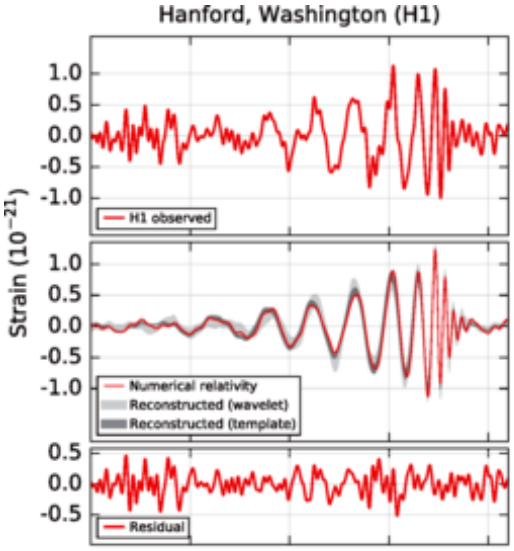

Abbott *et al.*, PRL **116**, 221101 (2016)

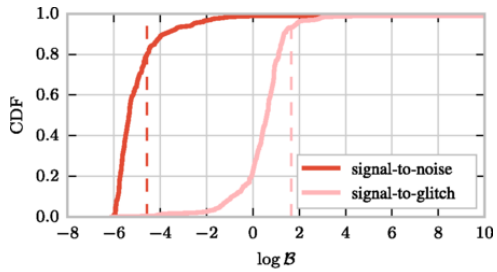

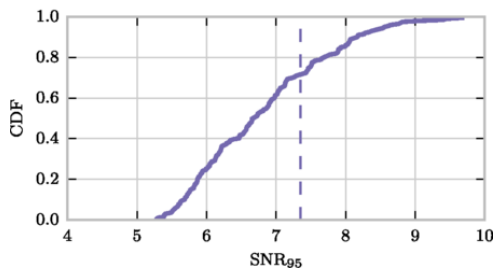

Inspiral-merger-ringdown consistency test

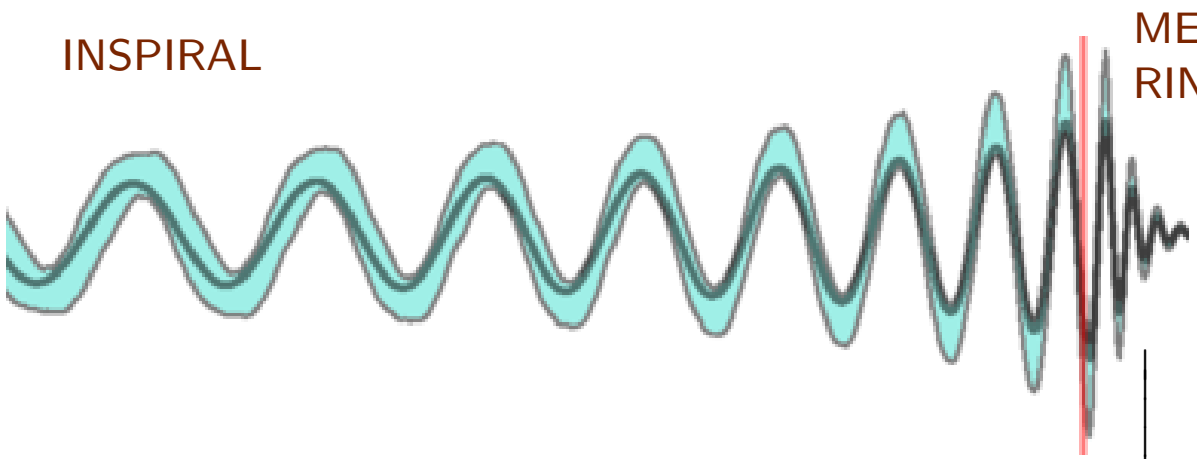

Final mass and spin

COMPARE!

NR fit

Initial masses and spins ⟶

Independent prediction of final mass and spin

Inspiral-merger-ringdown consistency test

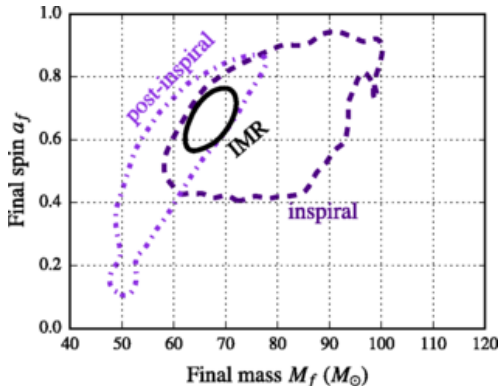

GW150914

Abbott *et al.*, PRL **116**, 221101 (2016)

Abbott *et al.*, PRL **118**, 221101 (2017)

GW150914 + GW170104

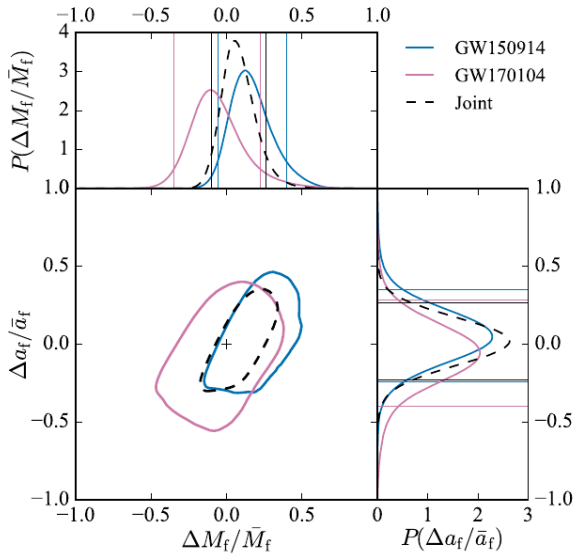

Mass and spin of the remnant object estimated from the inspiral and merger-ringdown parts agree with each other given GR predictions.

Ghosh *et al.* (2016); Ghosh *et al.* (2017)

Might not have been true in modified GR.

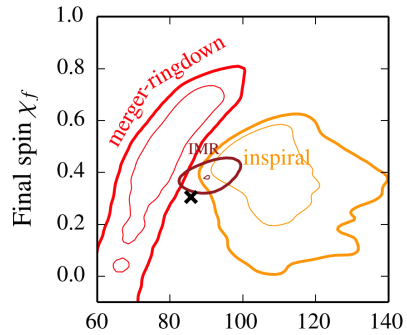

RAPID COMMUNICATIONS

PHYSICAL REVIEW D **94,** 021101(R) (2016)

Testing general relativity using golden black-hole binaries

Abhirup Ghosh,[1] Archisman Ghosh,[1] Nathan K. Johnson-McDaniel,[1] Chandra Kant Mishra,[1] Parameswaran Ajith,[1] Walter Del Pozzo,[2] David A. Nichols,[3] Yanbei Chen,[4] Alex B. Nielsen,[5] Christopher P. L. Berry,[2] and Lionel London[6]

Stronger constraints on systematic departures from GR combining information from multiple detections.

Inspiral-merger-ringdown consistency test

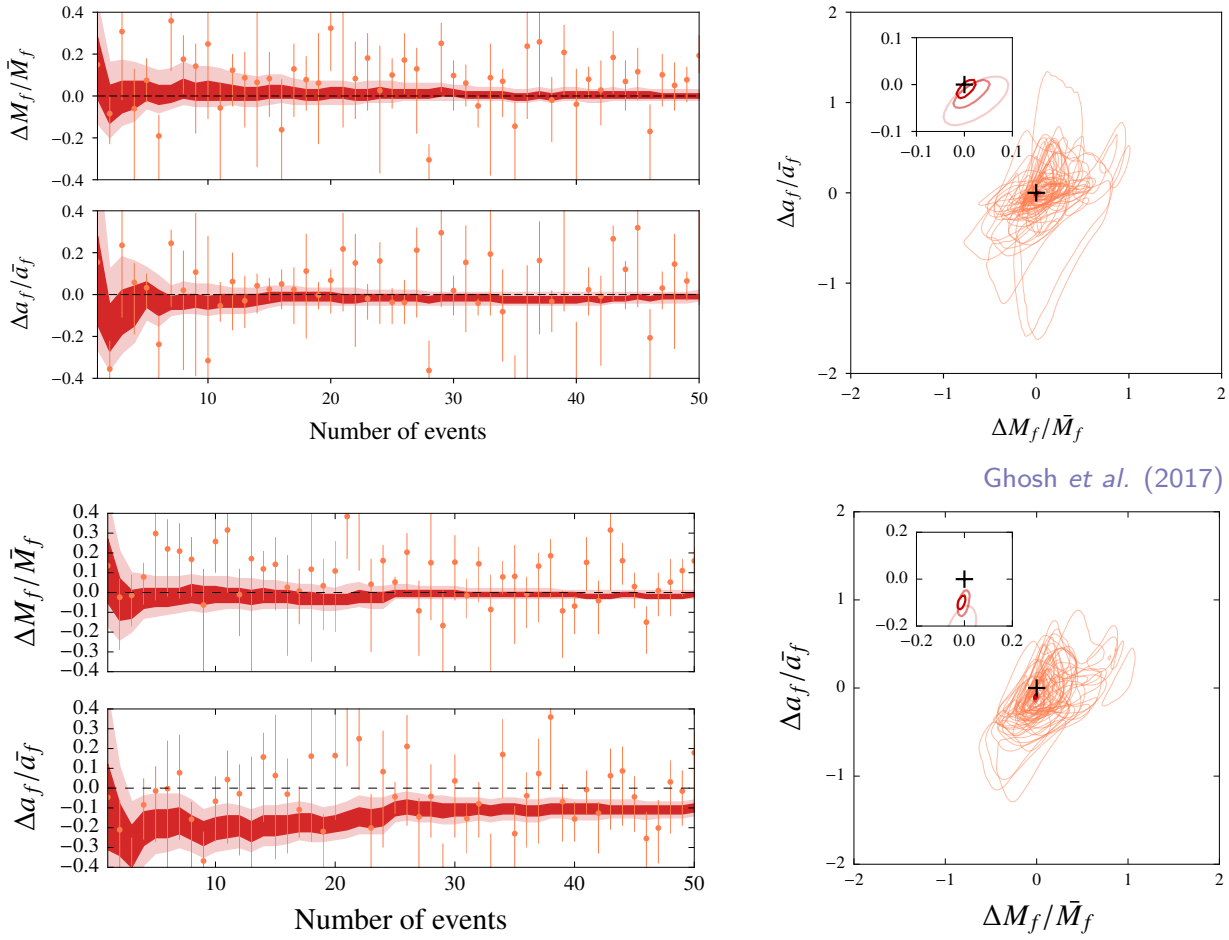

Ghosh *et al.* (2017)

Stronger constraints on systematic departures from GR combining information from multiple detections.

Parametrised tests of GR

- GW waveforms are expressed in terms of effective series, for the Phenom family:

$$h(f;\theta) = A(f;\theta)e^{i\Phi(f;\theta)}$$

$$\Phi(f;\theta) = \sum_{k=0}^{7}(\varphi_k + \varphi_k^{(l)})f^{(k-5)/3} + \sum_{i\neq k}\varphi_i g(f)$$

post-Newtonian series effective series

$$\varphi_j \equiv \varphi_j(m_1, m_2, \vec{s}_1, \vec{s}_2)$$

- Modified theories of gravity change the series (e.g. PPE: Yunes & Pretorius, arXiv:0909.3328, Cornish+,arXiv: 1105.2088)

- Perturb the GW phase around GR (Li+,arXiv:1110.0530, Agathos+,arXiv:1311.0420)

$$\hat{\varphi}_j \equiv \varphi_j^{GR}(1 + \delta\hat{\varphi}_j) \qquad \delta\hat{\varphi}_j = 0 \iff \text{GR}$$

- Bound violations by computing posterior distributions for the $\delta\hat{\varphi}_j$ in concert with the physical parameters of the system

waveform regime	parameter	$f-$dependence	
early-inspiral regime	$\delta\hat{\varphi}_0$	$f^{-5/3}$	post-Newtonian
	$\delta\hat{\varphi}_1$	$f^{-4/3}$	
	$\delta\hat{\varphi}_2$	f^{-1}	
	$\delta\hat{\varphi}_3$	$f^{-2/3}$	
	$\delta\hat{\varphi}_4$	$f^{-1/3}$	
	$\delta\hat{\varphi}_{5l}$	$\log(f)$	
	$\delta\hat{\varphi}_6$	$f^{1/3}$	
	$\delta\hat{\varphi}_{6l}$	$f^{1/3}\log(f)$	
	$\delta\hat{\varphi}_7$	$f^{2/3}$	
intermediate regime	$\delta\hat{\beta}_2$	$\log f$	effective
	$\delta\hat{\beta}_3$	f^{-3}	
merger–ringdown regime	$\delta\hat{\alpha}_2$	f^{-1}	
	$\delta\hat{\alpha}_3$	$f^{3/4}$	
	$\delta\hat{\alpha}_4$	$\tan^{-1}(af+b)$	

LVC, arXiv:1602.03841

Constraints on parameterized deformations from GR

Allowing coefficients in waveform models to deviate from their GR values, the deviation parameters do not show any departure from their GR values.

Li *et al.* (2011); Agathos *et al.* (2013); Meidam (PhD thesis, 2017); Meidam *et al.* (2017)

GW150914 + GW151226 + GW170104

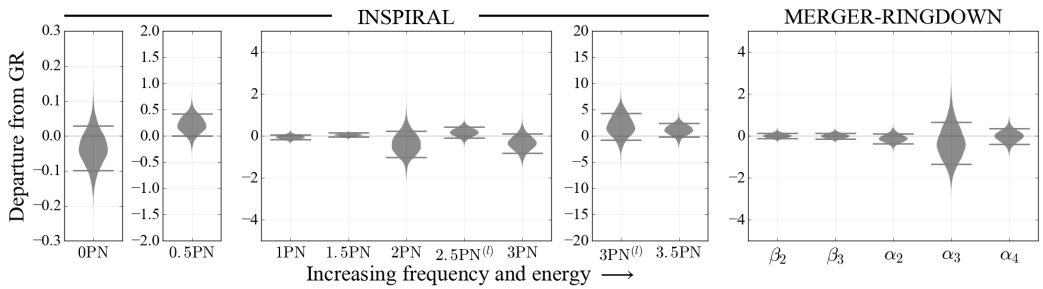

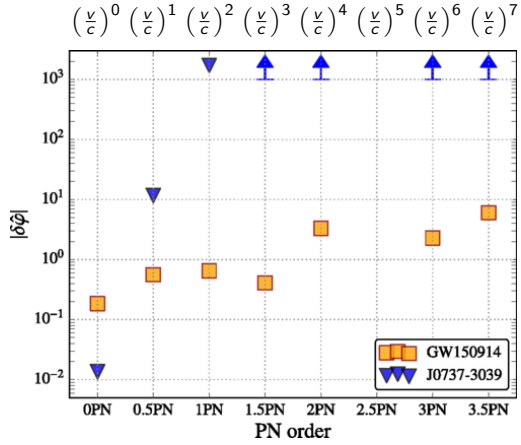

GW150914

Abbott *et al.*, PRL **116**, 221101 (2016)

Abbott *et al.*, PRL **118**, 221101 (2017)

First-ever measurement of orbital dynamics beyond leading order in v/c.

Deviation in $\left(\frac{v}{c}\right)^3$ coefficient constrained to $\mathcal{O}(10\%)$

Dynamical self-interaction of spacetime

Spin-orbit interaction

Constraints from modified dispersion

Will (1998); Mirshekari *et al.* (2012)

Modified dispersion relation:

(different frequencies travel with different speeds)

$$E^2 = p^2c^2 + \mathbb{A}\, p^\alpha c^\alpha$$

$$\lambda_{\mathbb{A}} \equiv hc\mathbb{A}^{1/(\alpha-2)}$$

$\alpha \neq 0 \quad \rightarrow \quad$ local Lorentz invariance violation

$\alpha = 0 \quad \rightarrow \quad$ massive graviton (for $\mathbb{A} > 0$)

GW150914 + GW151226 + GW170104

$$\lambda_g \equiv \frac{h}{m_g c} > 1.6 \times 10^{13}\text{km}$$

$$m_g < 7.7 \times 10^{-23}\text{eV}/c^2$$

Effect gets enhanced with propagation over a distance!

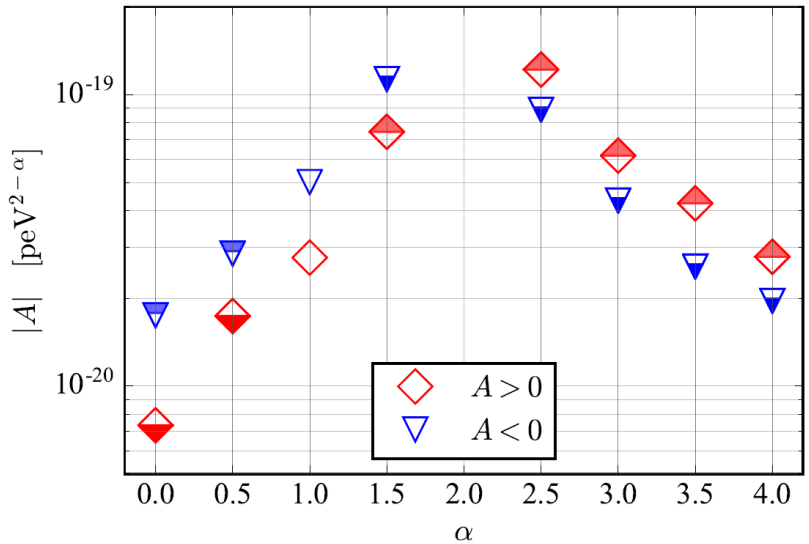

GW150914 + GW151226 + GW170104
Abbott *et al.*, PRL **118**, 221101 (2017)

TABLE III. 90% credible level lower bounds on the length scale λ_A for Lorentz invariance violation test using GW170104 alone. **GW170104**

	$A > 0$	$A < 0$
$\alpha = 0.0$	1.3×10^{13} km	6.6×10^{12} km
$\alpha = 0.5$	1.8×10^{16} km	6.8×10^{15} km
$\alpha = 1.0$	3.5×10^{22} km	1.2×10^{22} km
$\alpha = 1.5$	1.4×10^{41} km	2.4×10^{40} km

Agathos (PhD thesis, 2016); Samajdar (PhD thesis, 2017); Samajdar & Arun (2017)

Hubble scale $\approx 1.3 \times 10^{23}$km

Theoretical mechanism	GR pillar	PN	$\lvert\beta\rvert$		Example theory constraints			
			GW150914	GW151226	Repr. parameters	GW150914	GW151226	Current bounds
Scalar field activation	SEP	-1	$\mathbf{1.6\times10^{-4}}$	$\mathbf{4.4\times10^{-5}}$	$\sqrt{\lvert\alpha_{\rm EdGB}\rvert}$ [km]	$\cdots$	$\cdots$	10^{7} [60], 2 [61–63]
					$\lvert\dot{\phi}\rvert$ [1/ sec]	$\cdots$	$\cdots$	10^{-6} [64]
Scalar field activation	SEP, PI	$+2$	$\mathbf{1.3\times10^{1}}$	$\mathbf{4.1}$	$\sqrt{\lvert\alpha_{\rm dCS}\rvert}$ [km]	$\cdots$	$\cdots$	10^{8} [65,66]
Vector field activation	SEP, LI	0	$\mathbf{7.2\times10^{-3}}$	$\mathbf{3.4\times10^{-3}}$	(c_+, c_-)	$(\mathbf{0.9}, \mathbf{2.1})$	$(\mathbf{0.8}, \mathbf{1.1})$	(0.03,0.003) [67,68]
					$(\beta_{\rm KG}, \lambda_{\rm KG})$	$(\mathbf{0.42}, -)$	$(\mathbf{0.40}, -)$	(0.005,0.1) [67,68]
Extra dimensions	4D	-4	$\mathbf{9.1\times10^{-9}}$	$\mathbf{9.1\times10^{-11}}$	ℓ [μm]	$\mathbf{5.4\times10^{10}}$	$\mathbf{2.0\times10^{9}}$	10–10^{3} [69–73]
Time-varying G	SEP	-4	$\mathbf{9.1\times10^{-9}}$	$\mathbf{9.1\times10^{-11}}$	$\lvert\dot{G}\rvert$ [10^{-12}/yr]	$\mathbf{5.4\times10^{18}}$	$\mathbf{1.7\times10^{17}}$	0.1–1 [74–78]
Massive graviton	$m_g=0$	$+1$	$\mathbf{1.3\times10^{-1}}$	$\mathbf{8.9\times10^{-2}}$	m_g [eV]	$\mathbf{10^{-22}}$ [19]	$\mathbf{10^{-22}}$ [5]	10^{-29}–10^{-18} [79–83]
Mod. disp. rel.	LI	$+4.75$	$\mathbf{1.1\times10^{2}}$	$\mathbf{2.6\times10^{2}}$	E_*^{-1} [eV^{-1}] (time)	$\mathbf{5.8\times10^{-27}}$	$\mathbf{3.3\times10^{-26}}$	$\cdots$
(*multifractional*)					E_*^{-1} [eV^{-1}] (space)	$\mathbf{1.0\times10^{-26}}$	$\mathbf{5.7\times10^{-26}}$	3.9×10^{-53} [84]
Mod. disp. rel.	LI	$+5.5$	$\mathbf{1.4\times10^{2}}$	$\mathbf{4.3\times10^{2}}$	$\eta_{\rm dsrt}/L_{\rm Pl}>0$	$\mathbf{1.3\times10^{22}}$	$\mathbf{3.8\times10^{22}}$	$\cdots$
(*modified special rel.*)					$\eta_{\rm dsrt}/L_{\rm Pl}<0$			2.1×10^{-7} [84]
Mod. disp. rel.	4D	$+7$	$\mathbf{5.3\times10^{2}}$	$\mathbf{2.4\times10^{3}}$	$\alpha_{\rm edt}/L_{\rm Pl}^2>0$	$\mathbf{5.5\times10^{62}}$	$\mathbf{2.5\times10^{63}}$	2.7×10^{2} [84]
(*extra dim.*)					$\alpha_{\rm edt}/L_{\rm Pl}^2<0$			$\cdots$
		$+4$	$\cdots$	$\cdots$	$\overset{\circ}{k}{}^{(4)}_{(I)}>0$	$\cdots$	$\cdots$	6.1×10^{-17} [84,85]
					$\overset{\circ}{k}{}^{(4)}_{(I)}<0$	$\mathbf{0.64}$	$\mathbf{19}$	$\cdots$
Mod. disp. rel.	LI	$+5.5$	$\mathbf{1.4\times10^{2}}$	$\mathbf{4.3\times10^{2}}$	$\overset{\circ}{k}{}^{(5)}_{(V)}>0$ [cm]	$\mathbf{1.7\times10^{-12}}$ [86]	$\mathbf{3.1\times10^{-11}}$	1.7×10^{-40} [84,85]
(*standard model ext.*)					$\overset{\circ}{k}{}^{(5)}_{(V)}<0$ [cm]			$\cdots$
		$+7$	$\mathbf{5.3\times10^{2}}$	$\mathbf{2.4\times10^{3}}$	$\overset{\circ}{k}{}^{(6)}_{(I)}>0$ [cm^2]	$\mathbf{7.2\times10^{-4}}$	$\mathbf{3.3\times10^{-3}}$	3.5×10^{-64} [84,85]
					$\overset{\circ}{k}{}^{(6)}_{(I)}<0$ [cm^2]			$\cdots$
Mod. disp. rel.	LI	$+7$	$\mathbf{5.3\times10^{2}}$	$\mathbf{2.4\times10^{3}}$	$\kappa_{\rm hl}^4\mu_{\rm hl}^2$ [1/eV^2]	$\mathbf{1.5\times10^{6}}$	$\mathbf{6.9\times10^{6}}$	$\cdots$
(*Hořava-Lifshitz*)								
Mod. disp. rel.	LI	$+4$	$\cdots$	$\cdots$	c_+	$\mathbf{0.7}$ [87]	$\mathbf{0.998}$	0.03 [67,68]
(*Lorentz violation*)								

Yunes *et al.* (2016)

Polarization from 3-detector observation of GW170814

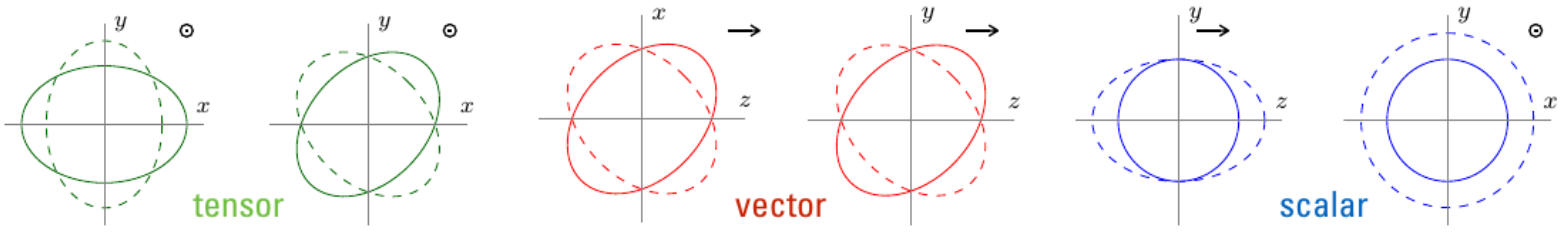

six polarizations $\longrightarrow$ distinct antenna patterns

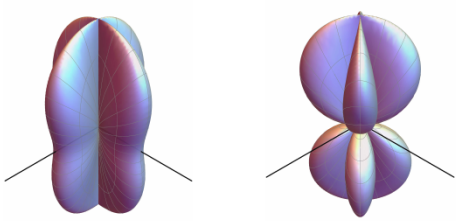
(a) Plus (+)

(b) Cross (×)

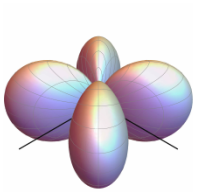
(c) Vector-x (x)

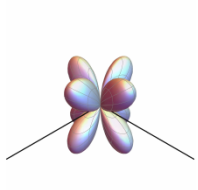
(d) Vector-y (y)


(e) Scalar (s)

$$|F^I_{\rm t}(\alpha,\delta)| \equiv \sqrt{F^I_+(\alpha,\delta)^2 + F^I_\times(\alpha,\delta)^2}\,,$$

$$|F^I_{\rm v}(\alpha,\delta)| \equiv \sqrt{F^I_{\rm x}(\alpha,\delta)^2 + F^I_{\rm y}(\alpha,\delta)^2}\,,$$

$$|F^I_{\rm s}(\alpha,\delta)| \equiv \sqrt{F^I_{\rm b}(\alpha,\delta)^2 + F^I_{\rm l}(\alpha,\delta)^2}$$

In GR: GW are transverse, traceless
only tensor polarizations

pure tensor / pure scalar = 1000 / 1
pure tensor / pure vector = 200 / 1

Isi & Weinstein (2017)

Need multiple detectors: **thanks to Virgo!**

Abbott *et al.*, PRL **119**, 141101 (2017)

Constraints from GW170817+GRB

Delay of only a few seconds after a propagation over one hundred million light years.

$$t_{\mathrm{EM}} - t_{\mathrm{GW}} = 1.74 \pm 0.05\,\mathrm{s}$$

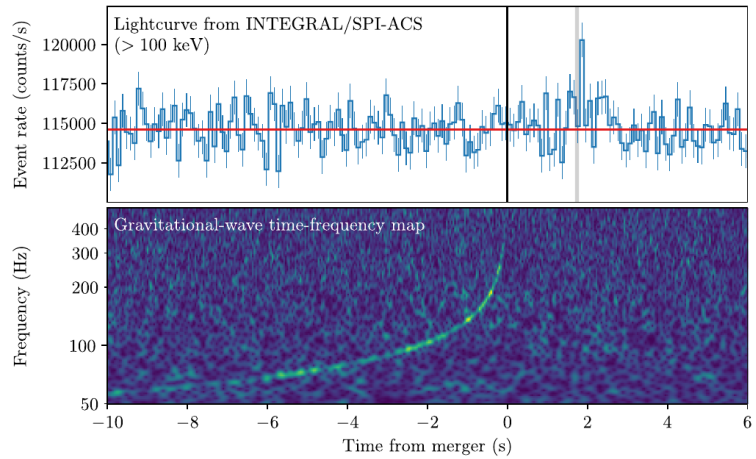

Constraints on speed of gravity assuming GRB emitted within 10s of GW

$$-3 \times 10^{-15} \leqslant \frac{v_{\mathrm{GW}} - v_{\mathrm{EM}}}{v_{\mathrm{EM}}} \leqslant +7 \times 10^{-16}$$

"Shapiro time delay" of GW and EM in the gravitational potential of our galaxy:

$$-2.6 \times 10^{-7} \leqslant \gamma_{\mathrm{GW}} - \gamma_{\mathrm{EM}} \leqslant 1.2 \times 10^{-6}$$

Test of the equivalence principle.

Abbott *et al.* Astrophys. J. **848** #2, L13 (2017)

GW170817

$$-3 \times 10^{-15} \leq \frac{\Delta v}{v_{EM}}{}^{*} \leq 7 \times 10^{-16}$$

$$S = \int d^4x\sqrt{-g}\Big\{K(\phi, X) - G_3(\phi, X)\Box\phi$$

$$+ G_4(\phi, X)R + G_{4,X}(\phi, X)\left[(\Box\phi)^2 - (\nabla_\mu\nabla_\nu\phi)(\nabla^\mu\nabla^\nu\phi)\right]$$

$$+ G_5(\phi, X)G_{\mu\nu}\nabla^\mu\nabla^\nu\phi - \frac{G_{5,X}(\phi, X)}{6}\left[(\Box\phi)^3 - 3\Box\phi(\nabla_\mu\nabla_\nu\phi)(\nabla^\mu\nabla^\nu\phi)\right.$$

$$\left. + 2(\nabla_\mu\nabla_\nu\phi)(\nabla^\mu\nabla_\sigma\phi)(\nabla^\nu\nabla^\sigma\phi)\right]\Big\}$$

Many models that could potentially explain the accelerated expansion yet evade solar system constraints via screening have been ruled out

Creminelli, Vernizzi, arXiv:1710.05877
Sakstein, Jain, arXiv:1710.05893
Baker et al, arXiv:1710.06394

* note that if gravity did not propagate at c, timing of binary pulsars would be impossible (Damour & Deruelle 81)

Tests of general relativity with GW170817

Dipole radiation

Abbott *et al.* arXiv:1811.00364 [gr-qc]

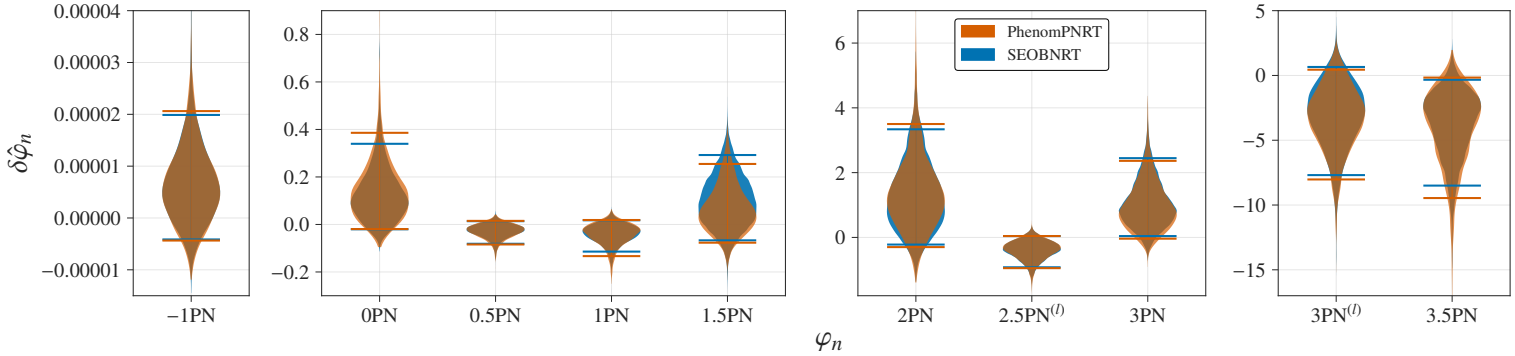

- Parameterized deviations do not show any departures from GR values.

- "Inverse square law" $\rightarrow$ constraints on extra dimensions.

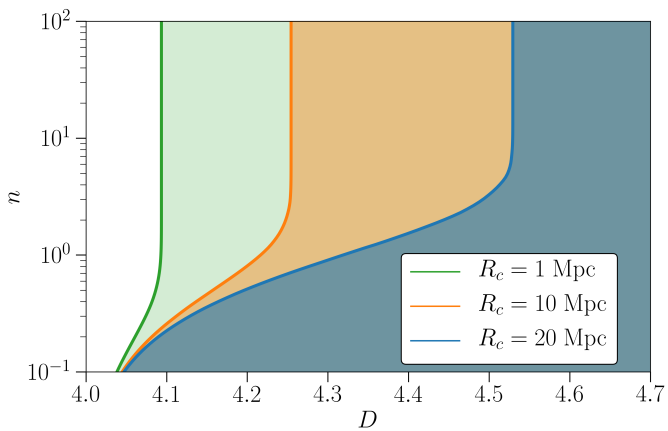

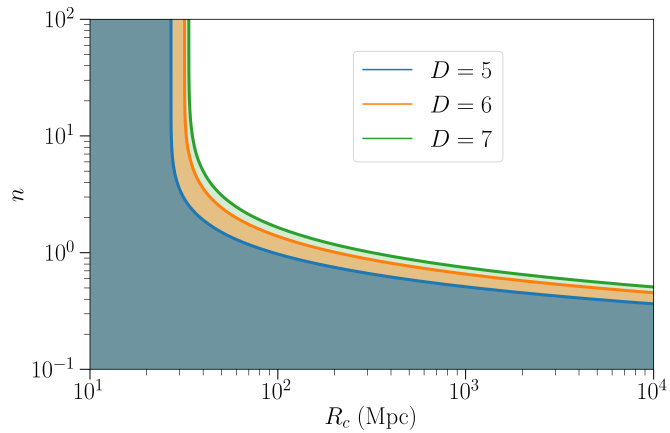

Expected improvement of results with more detections

- Additional detectors.

  Loudness scales as $\sqrt{N}_{\text{detectors}}$.

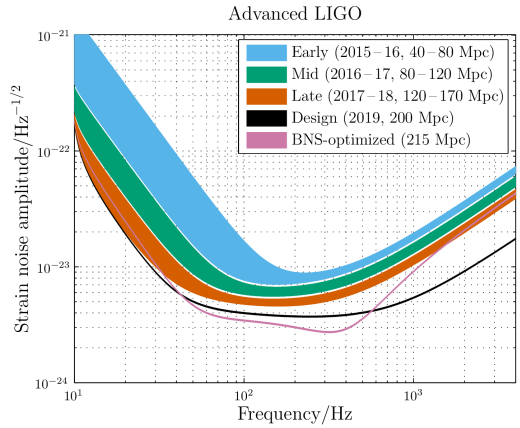

- Accuracies scale with detector sensitivity.

  For same event $3\times$ better at design sensitivity.

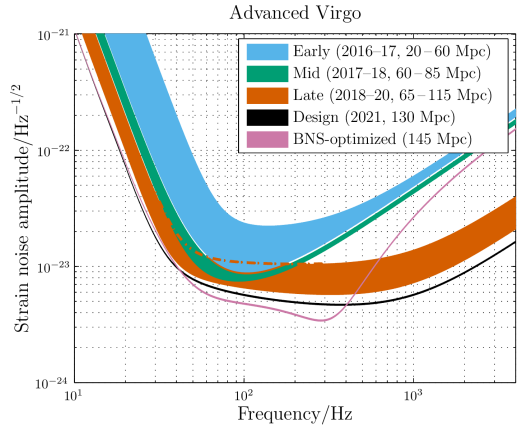

Amplitude detectors $\Rightarrow$ $27\times$ volume surveyed in same time

Abbott *et al.*, LLR (2016) 19:1

- Accuracies scale roughly with $\sqrt{N}_{\text{events}}$.

  After ~ 100 events, systematic deviations in $\left(\frac{v}{c}\right)^3$ constrained to 1% accuracy.

Dynamical self-interaction of spacetime

Spin-orbit interaction

Some prospects of doing better . . .

- Searching for systematic **systematic** departures.
- Is this the optimal way of testing?
- Use theoretically motivated combinations.

Multipole moments: Kastha *et al.* (2018)

- Use correlations between parameters.

Insights from simulations in modified gravity?

GW150914 + GW151226 + GW170104

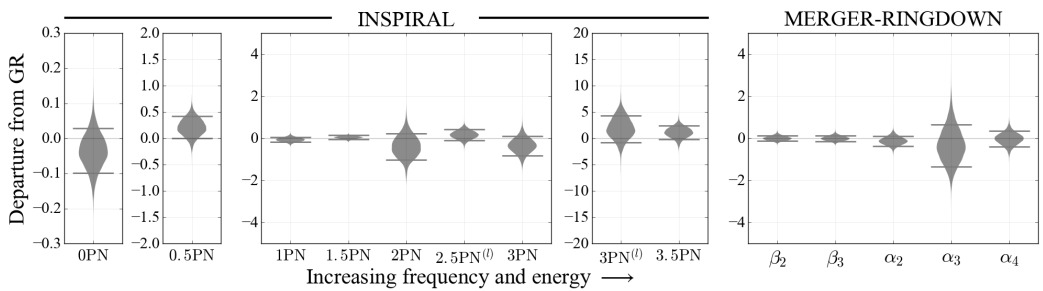

Abbott *et al.*, PRL **118**, 221101 (2017)

Probing the nature of the progenitor and remnant compact objects

Are they really black holes, or exotic compact objects mimicking black holes?

Boson stars, dark matter stars, gravastars, shells, wormholes

Three "complementary" ways in three different regimes:

- Finite size effects during inspiral.
- No-hair conjecture with quasinormal modes.
- Search for post-merger oscillations or "echoes".

Testing the no-hair conjecture with ringdown quasinormal modes

No-hair conjecture:

A stationary black hole in Einstein's general relativity is described only by its mass and spin.

During ringdown, the quasinormal mode frequencies and damping times will depend only on the mass and spin of the remnant black hole, which can be obtained from linearized Einstein equations on Kerr background.

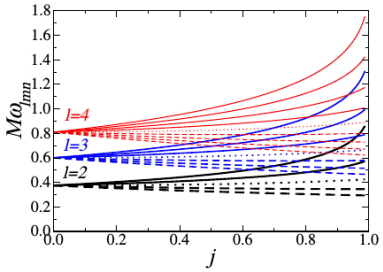

Berti *et al.* (2006)

$\Rightarrow$ Test for dependences $\omega_{lmn}(M_f, J_f)$, $\tau_{lmn}(M_f, J_f)$.

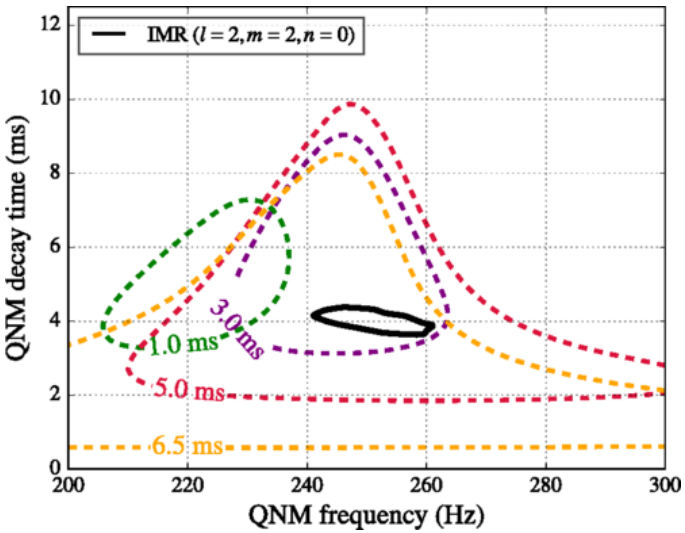

Difficult to measure leading QNM for GW150914.

Design sensitivity $\sim$ 3 times higher.

Abbott *et al.*, PRL **116**, 221101 (2016)

Testing the no-hair conjecture with ringdown quasinormal modes

Multiple approaches to study ringdown:

- "Coherent mode Stacking"

- TIGER-like test

Testing the no-hair conjecture with ringdown quasinormal modes

• Even where one is not able to isolate the individual modes, one can look for systematic departures in the QNM frequencies and damping times from their GR values.

Gossan *et al.* (2011) Meidam *et al.* (2014)

$$\omega_{lmn} = \omega^{GR}_{lmn}(1 + \delta\omega_{lmn}) \,, \quad \tau_{lmn} = \tau^{GR}_{lmn}(1 + \delta\tau_{lmn})$$

• The general expectation was that such tests would become effective only for sources detected by third generation or space-based detectors.

Empirical tests of the black hole no-hair conjecture using gravitational -wave observations

Gregorio Carullo,[1,2,*] Laura van der Schaaf,[2] Lionel London,[3] Peter T. H. Pang,[4] Ka Wa Tsang,[2] Otto A. Hannuksela,[4] Jeroen Meidam,[2] Michalis Agathos,[5] Anuradha Samajdar,[2] Archisman Ghosh,[2] Tjonnie G. F. Li,[4] Walter Del Pozzo,[1,6] and Chris Van Den Broeck[2,7]

- With $\mathcal{O}(5)$ BBH sources similar to GW150914, the systematic departures can be measured with an accuracy of $\sim 1.5\%$ by the Adv LIGO-Virgo at design sensitivity.

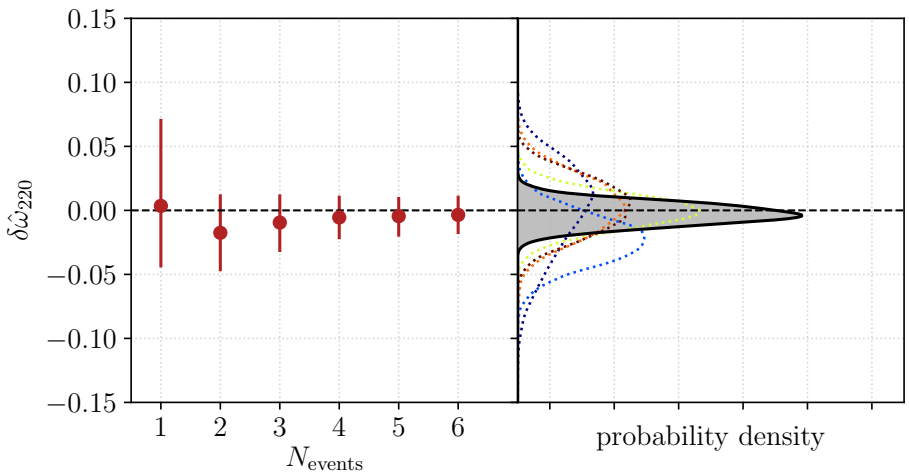

- Effective criterion for "start of ringdown" from point of view of parameter estimation.

Carullo *et al.* (2018)

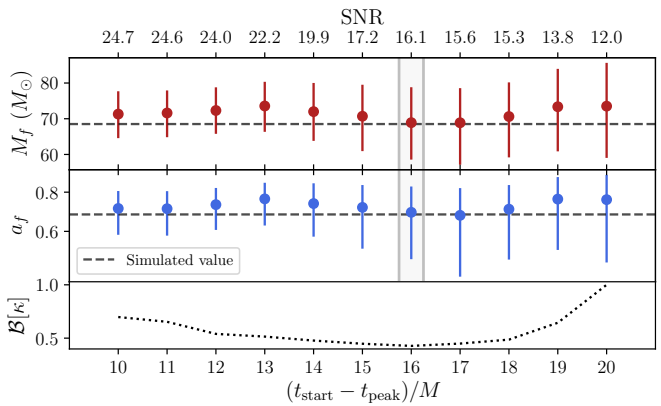

Search for "echoes" after the merger

In a large class of exotic compact objects,

Horizon-scale corrections $\Rightarrow$ secondary bursts of radiation.

Modulated and distorted train of "echoes".

$$\Delta t = nM \log(M/l)$$

n=8: wormholes

n=4: empty shell

n=6: thin-shell gravastars

Planck-scale corrections can appear relatively soon.

For an event like GW150914, $\Delta t = \mathcal{O}(100\,\mathrm{ms})$, at aLIGO design can hope to see first few echoes.

Can search for "echoes" immediately following the binary-merger detection.

Cardoso *et al.* (2016)

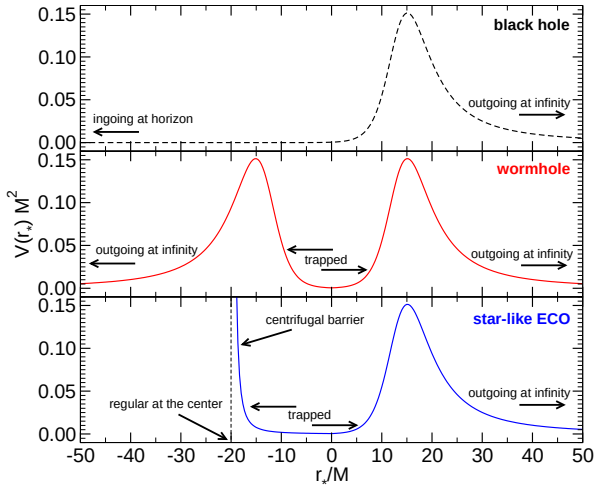

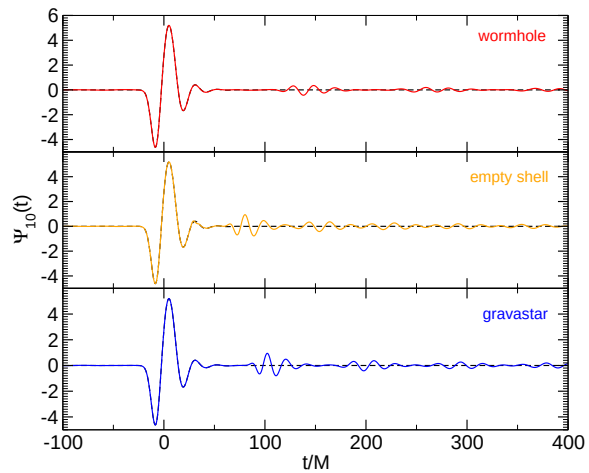

Not sufficiently modelled; Exotic objects not envisaged in literature.

One feature expected to be reasonably robust: constancy of time difference between the subsequent echoes.

A morphology-independent data analysis method for detecting and characterizing gravitational wave echoes

Ka Wa Tsang,[1] Michiel Rollier,[1] Archisman Ghosh,[1] Anuradha Samajdar,[1] Michalis Agathos,[2] Katerina Chatziioannou,[3] Vitor Cardoso,[4] Gaurav Khanna,[5] and Chris Van Den Broeck[1,6]

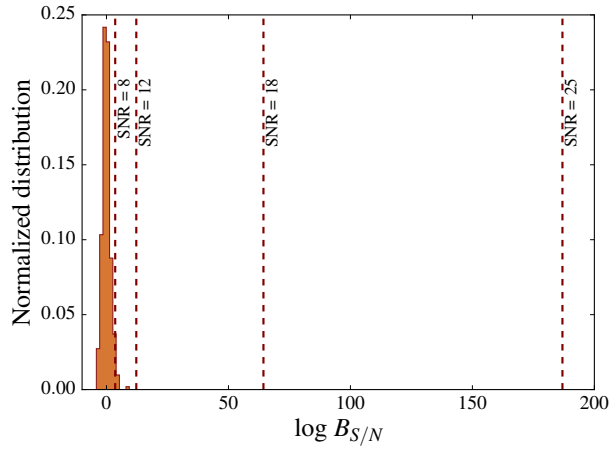

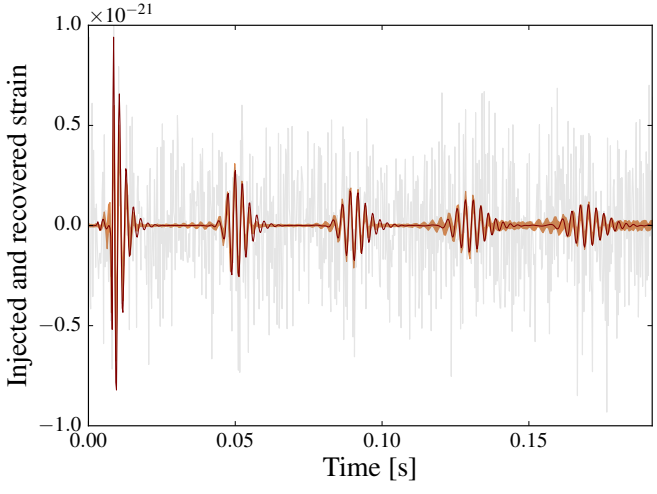

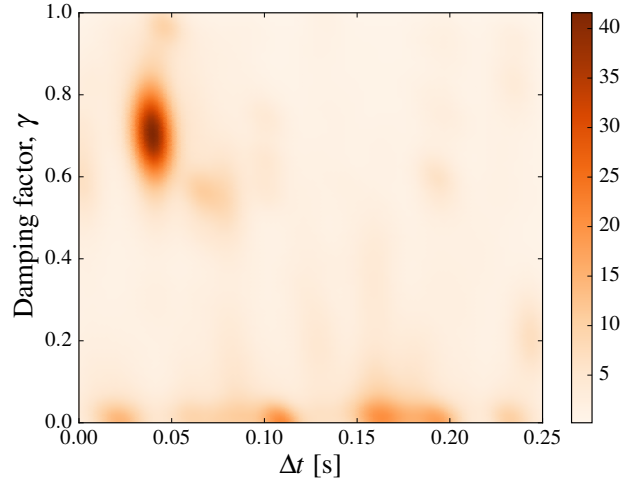

Conclusions and outlook

More and louder detections

New tests:

- More theoretically motivated searches?
- "Null stream" test for polarization
- Observation of ringdown

  Multiple efforts
- Searches for exotic behaviour

  Model-dependent and model-agnostic approaches

LIGO-VIRGO Joint Run Planning Committee

Working schedule for O3

(Public document G1801056-v4, based on G1800889-v7)